

# On the Homophily of Heterogeneous Graphs: Understanding and Unleashing

Zhen Tao<sup>1</sup>, Ziyue Qiao<sup>2</sup>, Chaoqi Chen<sup>3</sup>, Zhengyi Yang<sup>4</sup>, Lun Du<sup>5</sup>, Qingqiang Sun<sup>2\*</sup>

<sup>1</sup>Nanjing University, Nanjing, China <sup>2</sup>Great Bay University, Dongguan, China

<sup>3</sup>Shenzhen University, Shenzhen, China <sup>4</sup>University of New South Wales, Sydney, Australia

<sup>5</sup>Ant Research, Beijing, China

zhentao@smail.nju.edu.cn, ziyuejoe@gmail.com, cqchen1994@gmail.com,

zhengyi.yang@unsw.edu.au, dulun.dl@antgroup.com, qqsun@gbu.edu.cn

**Abstract**—Homophily, the tendency of similar nodes to connect, is a fundamental phenomenon in network science and a critical factor in the performance of graph neural networks (GNNs). While existing studies primarily explore homophily in homogeneous graphs, where nodes share the same type, real-world networks are often more accurately modeled as heterogeneous graphs (HGs) with diverse node types and intricate cross-type interactions. This structural diversity complicates the analysis of homophily, as traditional homophily metrics fail to account for distinct label spaces across node types. To address this limitation, we introduce the Cross-Type Homophily Ratio, a novel metric that quantifies homophily based on the similarity of target information across different node types. Furthermore, we introduce Cross-Type Homophily-guided Heterogeneous Graph Pruning, a method designed to selectively remove low-homophily cross-type edges, thereby enhancing the Cross-Type Homophily Ratio and boosting the performance of heterogeneous graph neural networks (HGNNs). Extensive experiments on five real-world HG datasets validate the effectiveness of our approach, which delivers up to 13.36% average relative performance improvement for HGNNs, offering a fresh perspective on cross-type homophily in heterogeneous graph learning.

**Index Terms**—heterogeneous graph neural network, homophily ratio, graph pruning

## I. INTRODUCTION

Homophily, the tendency for similar nodes to connect, is a well-studied phenomenon in network science [1]–[4], encapsulated by the principle that “birds of a feather flock together.” [5] This concept has been widely explored in relation to graph neural networks (GNNs), with studies indicating that traditional GNN models tend to perform better on graphs exhibiting high homophily [6]–[10]. Typically, homophily is defined in the context of homogeneous graphs, where it is based on the similarity of node labels [6], [9], [11]. However, real-world networks are often better represented as heterogeneous graphs (HGs) comprising multiple types of nodes and edges to capture complex relationships [12]. In HGs, the diverse label spaces across node types make it difficult to apply conventional homophily definitions. We demonstrate in subfigures (a) and (b) of Fig. 1 that existing methods can only measure homophily through label relevance among target-type nodes, while cross-type homophily between nodes of different types in HGs remains unmeasured. Due

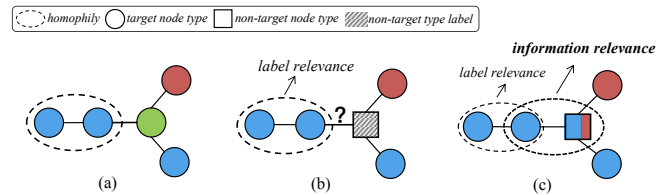


Fig. 1: Graph homophily in diverse cases where colors denote node labels: (a) the homophily in homogeneous graphs is considered based on node labels; (b) in heterogeneous graphs, label-relevance-based methods can only assess same-type homophily while failing to measure cross-type homophily; (c) our method is capable of evaluating cross-type homophily in heterogeneous graphs by leveraging information relevance.

to the prevalence of cross-type edges in HGs, relying solely on label relevance between connections of target-type nodes cannot fully capture the homophily in HGs, highlighting a significant gap between current work on homogeneous graphs and heterogeneous graphs.

Existing studies on HGs have shown that heterophily - or low homophily - can substantially impact the performance of heterogeneous graph neural networks (HGNNs) [10], [13], [14]. However, most prior work simplifies the structure of HGs by analyzing homophily only within same-type connections [13], [14]. This oversimplification overlooks a critical aspect: cross-type edges, which represent connections between different node types, are often predominant in real-world HGs and can play a decisive role in network dynamics and information flow. In real-world HGs, cross-type edges often constitute a significant proportion of the connections, underscoring their critical role in determining the structural properties of the graph. The potential value of studying homophily from a cross-type perspective lies in its ability to uncover deeper insights into node relationships in HGs, providing supplementary label information to improve label assignment and classification. For example, in e-commerce platforms, this approach can analyze user-product interactions through shared attributes, such as product categories or brands, facilitating more precise and informative node labeling. This enriched labeling enhances classification accuracy and supports the development of more

\*Corresponding author

effective recommendation systems. In HGs, the diversity of cross-type edges poses difficulties for analysis and processing, while their connection patterns significantly affect the information propagation of target-type nodes, which is pivotal for understanding the dissemination of target information. This paper addresses the homophily problem in HGs by focusing on cross-type edges, proposing a novel perspective on cross-type homophily. To the best of our knowledge, this study is the first to investigate homophily in HGs from this angle and offer an effective solution.

We identify two fundamental questions that address the challenges in homophily research for heterogeneous graphs: 1) *How to formulate and understand cross-type homophily in heterogeneous graphs?* 2) *How to effectively and efficiently harness the cross-type homophily to enhance the performance of HGNNs?*

Based on the challenges outlined above, our work defines a metric for measuring cross-type homophily in HGs. We also propose a graph pruning method, called **CTHGP** (**C**ross-**T**ype **H**omophily-guided **H**eterogeneous **G**raph **P**runing), to enhance the Cross-Type Homophily Ratio of HGs and improve the performance of HGNNs.

Specifically, to address the first challenge, we define Cross-Type Homophily Ratio (CHR) by target information, which distinguishes from traditional homophily metrics and quantifies homophily ratio between cross-type edges in HGs for the first time. As shown in Fig. 1, unlike (a) and (b), subfigure (c) illustrates our method, which can quantify cross-type homophily between nodes of different types in HGs through information relevance. Cross-type homophily broadens the scope of homophily research while also providing new perspectives for understanding the complex structures of HGs. In our initial research, we first revisit the original concept of homophily [5]. Subsequently, we conducted an analysis of homophily in HGs. Building on the principle of similarity-driven connections, we proposed the concept of cross-type homophily. To quantify this phenomenon, we leverage target labels as a measure of target information and introduce a target information propagation process, enabling non-target nodes to acquire this information. The CHR is then computed based on the similarity of the propagated target information.

To understand the cross-type homophily ratio, we conducted both theoretical analyses and empirical validations. Theoretically, we analyzed and established the relationship between CHR and the generalization of HGNNs, demonstrating that an increase in CHR improves the generalization lower bound of HGNNs. This finding highlights the potential of CHR in enhancing HGNN performance. Empirically, we constructed HGs with varying CHR values and explored the practical relationship between CHR and HGNN performance using a unified model. The results further confirmed the positive correlation between CHR and HGNN performance.

To address the second challenge, we propose the Cross-Type Homophily-guided Heterogeneous Graph Pruning (CTHGP) method. Specifically, building on our proposed CHR definition, CTHGP leverages a graph pruning strategy to enhance the

CHR of HGs, aiming to improve the performance of HGNN. By removing cross-type edges with low CHR, CTHGP refines the structure of HGs, thereby increasing CHR and boosting HGNN effectiveness. By propagating target information and clustering similar nodes, CTHGP strengthens information interactions and produces more relevant node representations. Complexity analysis demonstrates its computational efficiency. As a plug-and-play framework, CTHGP can be seamlessly integrated with various HGNN models. The pruned HGs generated by CTHGP directly enhance CHR and can be fed into HGNNs without additional adjustments, significantly improving node classification performance. Experiments conducted on five real-world HG datasets validate the effectiveness and adaptability of CTHGP.

In summary, our contributions are as follows:

- To the best of our knowledge, we are the first to investigate the homophily problem in HGs through cross-type edges. We conduct a detailed analysis of homophily in HGs, define the concept of Cross-Type Homophily, and introduce CHR as a novel metric to measure cross-type homophily in HGs.
- To further understand CHR, we conduct both theoretical analyses and empirical evaluations. Through generalization proofs and empirical validation, we investigate the connection between the CHR of HGs and the performance of HGNNs, providing a comprehensive understanding of CHR.
- We propose CTHGP, an efficient heterogeneous graph pruning method that selectively removes low CHR cross-type edges to refine the structure of HGs. Designed as a versatile, plug-and-play framework, CTHGP seamlessly integrates with various HGNN architectures while ensuring computational efficiency and maintaining low complexity.
- We conduct extensive experiments on five heterogeneous graph datasets using seven HGNN backbones. The results demonstrate the effectiveness of CTHGP which boosts the performance of diverse HGNNs by margins of up to 13.36% across all datasets, making it a promising tool for heterogeneous graph refinement.

## II. RELATED WORK

### A. Heterogeneous Graph Neural Networks

Recent progress in heterogeneous graph neural networks (HGNNs) [15] has yielded significant advancements, which can be broadly classified into meta-path-based approaches [16], [17] and meta-path-free methods [18], [19].

Meta-path-based HGNNs utilize predefined meta-paths to structure graph relationships. HAN [20] converts an HG into homogeneous subgraphs and integrates their representations with attention mechanisms. MAGNN [21] retains intermediate nodes that HAN excludes. These methods necessitate manual meta-path selection. GTN [22] automates meta-path generation with learnable relation weights and matrix multiplication, while MEGNN [23] enhances GTN’s efficiency by optimizing

matrix operations. Meta-path-free HGNNs working directly on HGs through message-passing and aggregation processes. RGCN [24] performs neighbor aggregation based on edge types, while HetSANN [25] employs type-specific attention for localized aggregation. HGT [26] adopts a Transformer-like encoder with parameters specific to node and edge types. Simple-HGN [18] extends the GAT model by incorporating edge-type-specific attention. HetGNN [27] samples neighbors through random walks with restarts and applies type-level attention for aggregation, while HINormer [28] combines a local structural encoder and a heterogeneous relation encoder with GATv2 [29] to effectively capture both structural and heterogeneous information for enhanced node representation. These studies have primarily concentrated on designing HGNNs to effectively process HGs, they have paid little attention to identifying the characteristics of HGs that are particularly beneficial for these models. Our work explores the properties of HGs that enhance the performance of existing HGNNs.

### B. Heterophily in Graph Neural Networks

The lack of homophily, referred to as heterophily [7], has been recognized as a key limitation to GNN performance. In response, recent works have introduced a variety of analyses, benchmarks, and models aimed at improving GNN capabilities under heterophily [10], [30]–[34]. Notable approaches include Geom-GCN [6], which uses network embeddings to construct structured neighborhoods, segmenting them into geometric blocks for distinct aggregation. FAGCN [30] applies a self-gating mechanism to balance low- and high-frequency signals, while GBK-GNN [35] consider positive and negative correlations, using block similarity to adjust edge weights. UGCN [36] introduce ranking-based aggregation and GloGNN [37] integrate global node information.

Research on heterophily for homogeneous graphs have been extensively studied, yet evaluating homophily in HGs remains challenging due to the diversity of node types and interactions. This complexity underscores the need for novel metrics and representation learning techniques specifically designed for HGs [10]. Several studies have explored the issue of heterophily in HGs [38]–[40]. HDHGR [13] introduces a meta-path-based metric to quantify homophily in HGs, while Hetero2Net [14] employs meta-path-based label homophily and Dirichlet energy to evaluate heterophily. However, these methods primarily extend principles designed for homogeneous graphs, and research on heterophily metrics that account for the unique structural characteristics of HGs remains limited. Specifically, existing studies have largely overlooked the issue of homophily across cross-type nodes in HGs. In this work, we address this gap by proposing, for the first time, a method that effectively handles homophily across cross-type nodes, providing a novel approach tailored for HGs.

### C. Graph Structure Learning and Graph Pruning

Graph structure learning (GSL) methods [41]–[44] have been developed to refine graph structures derived from noisy

data, with the objective of uncovering more accurate underlying relationships. Typically, GSL frameworks adjust node connections through consistent approaches, broadly classified into metric learning [42], [45], [46], probabilistic modeling [43], [47], and direct optimization [41], [48]. Some GSL models address more complex scenarios; for example, HGSL [49] extends GSL applications to HGs, while SUBLIME [44] employs contrastive learning to align graph structures with adaptive, self-improving objectives. Graph rewiring is a prominent approach aimed at refining graph connectivity, thereby improving training and inference efficiency. [13], [50], [51]. Similarly, graph pruning (GP) techniques improve GNN performance by sparsifying graph structures to retain only essential edges, which preserves core connectivity and minimizes noise, optimizing storage and performance in downstream tasks [47], [52], [53]. Notable examples include DropEdge [52], a GP method that randomly removes edges to mitigate the over-smoothing issue in deep GNNs, and NeuralSparse [47], which leverages task-specific feedback from downstream objectives to retain relevant edges. STEP [53] offers a self-supervised approach for pruning large-scale dynamic graphs, facilitating adaptive structure learning for streaming data without explicit message passing. In this paper, our method performs graph pruning by evaluating edge similarity to selectively remove edges while retaining key connections.

## III. PRELIMINARY CONCEPTS AND MOTIVATION

### A. Preliminary Concepts

#### Definition 1. Heterogeneous Graph.

A heterogeneous graph (HG) can be defined as  $\mathcal{G} = \{\mathcal{V}, \mathcal{E}, \phi, \psi\}$ , where  $\mathcal{V}$  is the set of nodes and  $\mathcal{E}$  is the set of edges. Each node  $v$  has a type  $\phi(v)$ , and each edge  $e$  has a type  $\psi(e)$ . The sets of possible node types and edge types are denoted by  $T_v = \{\phi(v) : \forall v \in \mathcal{V}\}$  and  $T_e = \{\psi(e) : \forall e \in \mathcal{E}\}$ .

According to the definition of HG, when  $|T_v| = |T_e| = 1$ , the graph simplifies to a homogeneous graph. The concept of the homophily ratio, traditionally defined for homogeneous graphs, measures the extent of homophily within the graph. Below, we provide the definition of the traditional homophily ratio in homogeneous graph.

#### Definition 2. Homophily Ratio of Homogeneous Graph.

Given a homogeneous graph  $\mathcal{G} = (\mathcal{V}, \mathcal{E})$ , homophily ratio is determined by the proportion of edges that connect nodes with identical labels, specifically among edges linking nodes of the same type. The homophily ratio  $H(\mathcal{G})$  is defined as:

$$H(\mathcal{G}) = \frac{\sum_{(v_i, v_j) \in \mathcal{E}} 1(y_i = y_j)}{|\mathcal{E}|} \quad (1)$$

where  $1(y_i = y_j)$  is an indicator function that returns 1 if nodes  $v_i$  and  $v_j$  have identical labels ( $y_i = y_j$ ), and 0 otherwise.  $y_i$  and  $y_j$  denote the labels of nodes  $v_i$  and  $v_j$ , respectively.  $|\mathcal{E}|$  represents the total number of edges that connect nodes of the same target type within the graph.

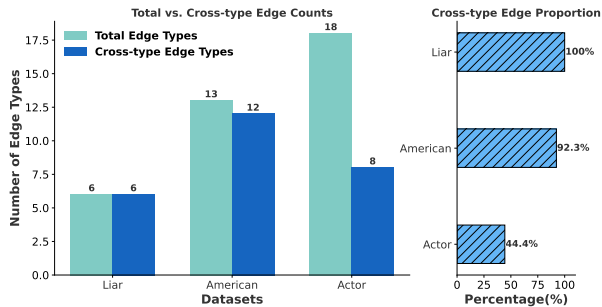


Fig. 2: Edge type distribution across different heterogeneous graphs. *Total Edge Types* represents the total number of edge types in each dataset, *Cross-type Edge Types* indicates the number of edge types connecting target-type nodes with non-target-type nodes, and *Percentage* shows the proportion of *Cross-type Edge Types* among the *Total Edge Types*. The proportion of *Cross-type Edge Types* among the edge types in HGs is significant.

The above definition represents the homophily ratio in homogeneous graphs. Subsequently, we conduct an analysis of the homophily problem in HGs and present our formal definition.

### B. Motivation of Cross-Type Homophily

Homophily, a concept introduced by Lazarsfeld and Merton [54], refers to the tendency of individuals to form connections with others who share similar attributes. In its original definition, homophily is observed as the tendency for nodes with similar properties to connect more easily [5]. When applied to homogeneous graphs, homophily is typically measured based on label similarity, using node labels as a criterion [6]. In HGs, which also contain nodes and edges, a significant proportion of edges are cross-type edges, as illustrated in Fig. 2, connecting nodes of diverse types. This diversity in node types makes it challenging to directly compare node labels, thereby complicating the measurement of homophily. As a result, the traditional definition of homophily cannot be directly applied to HGs.

To address this limitation, we propose the concept of cross-type homophily, which captures the tendency of nodes with different types in HGs to connect through shared dependencies or attributes. This concept extends traditional homophily to account for the structural and attribute diversity in HGs, offering a new perspective for analyzing HGs. For example, in e-commerce platforms, cross-type homophily is evident through shared attributes such as product categories or brands. A user’s preference for products within a specific category or brand reflects strong cross-type homophily with the corresponding product attributes. Using these shared attributes as supplementary label information enhances node labeling accuracy, improves classification performance, and supports the development of more effective recommendation systems.

We analyze cross-type homophily in HGs using the label information of target nodes, where the label serves both as

a classification indicator and a quantitative measure of cross-type homophily. This dual role establishes the relationship between target nodes and their surrounding non-target nodes. We hypothesize that non-target nodes inherently encode implicit target-related information through their connections with target nodes. By propagating information across cross-type edges, we analyze and normalize the distribution of target information around non-target nodes to define their label information, forming the foundation of our CHR metric. This approach enables us to quantify cross-type homophily in HGs and gain deeper insights into their structural properties.

## IV. UNDERSTANDING THE HOMOPHILY IN HGs

### A. Definitions about Cross-Type Homophily Ratio

An HG is characterized by the diversity of its node and edge types, which distinguishes it from a homogeneous graph. First, we classify the nodes in HGs into two types and divide the edge set into three distinct categories.

#### Definition 3. Node and Edge Types in Heterogeneous Graph.

In a heterogeneous graph, nodes are divided into **target nodes**  $\mathcal{V}_t$  and **non-target nodes**  $\mathcal{V}_n$ , with  $\mathcal{V} = \mathcal{V}_t \cup \mathcal{V}_n$ . The edge set is categorized into three types based on the node types they connect: (1) *intra-target edges*  $\mathcal{E}_{tt}$  between  $\mathcal{V}_t$ , (2) *cross-type edges*  $\mathcal{E}_{tn}$  between  $\mathcal{V}_t$  and  $\mathcal{V}_n$ , and (3) *intra-non-target edges*  $\mathcal{E}_{nn}$  between  $\mathcal{V}_n$ . Their adjacency matrices are denoted as  $\mathcal{A}_{tt}$ ,  $\mathcal{A}_{tn}$ ,  $\mathcal{A}_{nt}$ , and  $\mathcal{A}_{nn}$ , where subscripts indicate the types of nodes at each edge’s endpoints.

**Target Information.** The fundamental metric for evaluating CHR is target information. Specifically, for target nodes with known labels, the one-hot encoded labels represent their target information. For non-target nodes, target information is propagated from target nodes through cross-type edges, resulting in an information distribution referred to as target information. The construction of the target information matrix involves the following steps.

**Target Information Initialization.** For target nodes with known labels in the training set, denoted as  $v_i^{train} \in \mathcal{V}_{t-train}$ , their labels are defined as  $L(v_i^{train}) = \mathbf{e}_{y_i}$ , where  $y_i \in \{1, 2, \dots, C\}$  and  $\mathbf{e}_{y_i}$  is the one-hot vector for class  $y_i$  with  $C$  total classes. In real-world datasets, some target nodes lack label information. To enhance the reliability of information propagation, we assign these nodes a probabilistic label distribution. Using the original HG  $\mathcal{G}$ , we train an HGNN model parameterized by  $\theta$ , denoted as  $f_\theta$ , which outputs logits distributions  $f_\theta(\mathcal{G}, \mathcal{X}) \in \mathbb{R}^{N \times C}$ . For target nodes without known labels, denoted as  $v_i^{test} \in \mathcal{V}_{t-test}$ , their probabilistic label distribution is assigned based on the softmax-normalized output of the HGNN:

$$L(v_i^{test}) = \text{softmax}(f_\theta(\mathcal{G}, \mathcal{X})[v_i^{test}]) \in \mathbb{R}^C. \quad (2)$$

Here, the softmax operation normalizes the output logits into a probability distribution over  $C$  classes, capturing prediction uncertainty. Leveraging this distribution instead of a single label enhances the representation of confidence and reduces errors from hard label assignments, making the propagated

CHR Example

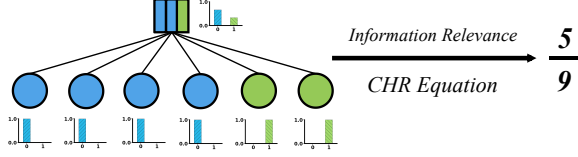


Fig. 3: Illustration of Cross-Type Homophily Ratio. Circles represent target-type nodes with colors indicating target labels, while squares represent non-target nodes. The bar chart shows the distribution of target information. By deriving the information distribution of a non-target node through neighboring nodes and applying Information Relevance, we calculate CHR using Equation 8, resulting in a value of  $\frac{5}{9}$ .

information more reliable and robust. Thus, the initial target information matrix for target nodes is given by  $L \in \mathbb{R}^{N_t \times C}$ .

**Target Information Propagation.** Target information is propagated to neighboring non-target nodes via cross-type edges  $\mathcal{E}_{tn}$ . For each non-target node  $v_i \in \mathcal{V}_n$ , the target information it receives from neighboring target nodes  $v_j \in \mathcal{V}_t$  is calculated as:

$$P_i = \sum_{v_j \in \mathcal{N}(v_i)} w_{ji} L_j \quad (3)$$

where  $w_{ji}$  represents the propagation strength of the edge, indicating the intensity of information transfer, and  $L_j$  is the target information of target node  $j$ . The overall target information propagation process is expressed as:

$$P = (\mathcal{W} \circ \mathcal{A}_{nt}) L \quad (4)$$

where  $P \in \mathbb{R}^{N_n \times C}$  is the information matrix for non-target nodes,  $N_n$  is the number of non-target nodes,  $\circ$  denotes the Hadamard product (element-wise multiplication), and  $\mathcal{W}$  is the edge propagation strength matrix, which is set based on the weight of each edge in the dataset. A potential direction for future research is to explore the configuration of  $\mathcal{W}$  and the setting of specific edge types. To ensure comparability between  $L$  and  $P$ , we normalize the propagated target information as follows:

$$P'_i = \frac{P_i}{\sum_{j=1}^C P_{ij}} \quad (5)$$

where  $P_{ij}$  represents the information for the  $i$ -th node regarding the  $j$ -th category.

The normalized target information matrix for non-target nodes  $P' \in \mathbb{R}^{N_n \times C}$  is concatenated with the target information matrix  $L \in \mathbb{R}^{N_t \times C}$  to form the final target information matrix:

$$I = \begin{bmatrix} L \\ P' \end{bmatrix} \in \mathbb{R}^{N \times C} \quad (6)$$

where  $N = N_t + N_n$  represents the total number of nodes. The target information matrix  $I \in \mathbb{R}^{N \times C}$  provides a quantitative foundation for assessing cross-type homophily between nodes.

#### Definition 4. Cross-Type Homophily Ratio.

The Cross-Type Homophily Ratio (CHR) measures the homophily between target nodes and non-target nodes in an HG using the target information matrix  $I \in \mathbb{R}^{N \times C}$ . For any target node  $v_i$  and non-target node  $v_j$  connected by an edge  $e_{ij} \in \mathcal{E}_m$ , the similarity of their target information is defined as the inner product of their respective target information vectors,  $I(v_i)$  and  $I(v_j)$ :

$$S_{ij} = \sum_{k=1}^C I(v_i)_k I(v_j)_k = I(v_i)^\top I(v_j) \quad (7)$$

The CHR in an HG is then calculated as:

$$CHR = \frac{\sum_{(v_i, v_j) \in \mathcal{E}_m} S_{ij}}{|\mathcal{E}_m|} \quad (8)$$

where the numerator represents the total similarity of target information between all pairs of target and non-target nodes, and the denominator  $|\mathcal{E}_m|$  denotes the total number of cross-type edges.

We present a simple example of CHR in Fig. 3. To further evaluate homophily, we extend the edge set to include cross-type and intra-target edges and propose the Extended Target Homophily Ratio, which quantifies the homophily of target information among nodes in HGs, including both target-target and target-non-target relationships.

#### Definition 5. Extended Target Homophily Ratio.

The Extended Target Homophily Ratio (HR) measures the degree of homophily related to target information in an HG. It is defined over the edge set  $\mathcal{E}_t \cup \mathcal{E}_m$ , which includes intra-target edges and cross-type edges involving target nodes. For any edge  $e_{ij}$  connecting nodes  $v_i$  and  $v_j$ , the target information similarity is denoted as  $S_{ij}$ , based on the target information matrix  $I \in \mathbb{R}^{N \times C}$ . The HR is calculated as:

$$HR = \frac{\sum_{(v_i, v_j) \in \mathcal{E}_t \cup \mathcal{E}_m} S_{ij}}{|\mathcal{E}_t \cup \mathcal{E}_m|} \quad (9)$$

where the numerator sums the similarity scores  $S_{ij}$  over all edges in  $\mathcal{E}_t \cup \mathcal{E}_m$ , and the denominator represents the total number of these edges.

#### B. Generalization Analysis of CHR and HGNNs

In this subsection, we theoretically examine the relationship between CHR and HGNNs. We evaluate the generalization capacity of HGNNs using the complexity measure (CM), with a particular focus on how cross-type homophily in graph data impacts generalization performance.

The Complexity Measure is defined as a function  $M : \{H, S\} \rightarrow \mathbb{R}^+$  that quantifies model complexity, where  $H$  denotes a class of models and  $S$  represents a training dataset. Lower complexity measure values suggest better generalization potential. Here, we specify  $H$  as meta-path-free HGNNs with different parameters and define  $S$  as HGs with designated Cross-Type Homophily Ratio. Various forms of CM exist; we use the Consistency of Representations approach [55], based

on the Davies-Bouldin index [56], to calculate it. For a given dataset and model layer, complexity measure is calculated as:

$$S_i = \left( \frac{1}{n_k} \sum_{t=1}^{n_i} |O_i^{(t)} - \mu_{O_i}|^p \right)^{\frac{1}{p}}, \quad i = 1, \dots, k \quad (10)$$

$$M_{i,j} = \|\mu_{O_i} - \mu_{O_j}\|_p, \quad i, j = 1, \dots, k \quad (11)$$

where  $i, j$  are category indices,  $O_i^{(t)}$  represents the embedding of the  $t$ -th instance in category  $i$ , and  $\mu_{O_i}$  is the centroid of category  $i$ . The intra-class distance  $S_i$  captures within-category variation, while  $M_{i,j}$  measures inter-class distance. The Davies-Bouldin index for CM is then calculated as:

$$C = \frac{1}{k} \sum_{i=0}^{k-1} \max_{i \neq j} \frac{S_i + S_j}{M_{i,j}} \quad (12)$$

Setting  $p = 2$  simplifies this metric to the ratio of intra-class variance to inter-class variance. Under this setting, we state the following theorem:

**Theorem 1.** *Let  $\mathcal{G} = (\mathcal{V}, \mathcal{E}, \phi, \psi)$  denote an HG. We consider a binary classification problem involving node classification with an HGNN across the entire graph  $\mathcal{G}$ . Using target information as the classification criterion, we model the distribution of non-target nodes as a spatial interpolation of the target node distributions. When Cross-Type Homophily reaches a maximum value of 1 (100%), the generalization capacity of the HGNN achieves its theoretical upper bound.*

*Proof.* To establish this theorem, we introduce the parameter  $Q_c$  to estimate the lower bound of the complexity measure  $C$  within a general heterogeneous graph convolutional layer. Employing principles from Consistency of Representations [55] and Fisher Discriminant Analysis [57], we utilize the ratio of intra-class variance to inter-class variance as a primary metric, reformulating the Consistency of Representations as a squared expression to enable rigorous theoretical validation:

$$C = \frac{1}{k} \sum_{t=0}^{k-1} \max_{t \neq s} \frac{T_t^2 + T_s^2}{M_{t,s}^2} \quad (13)$$

Our analysis focuses on node classification across HG by leveraging target information in a binary classification setting. For non-target nodes  $X_{nt}$ , their representations are expressed as a spatial mixture of target node distributions  $X_0$  and  $X_1$ :

$$\mu X_{nt} = \lambda \mu X_0 + (1 - \lambda) \mu X_1 \quad (14)$$

To account for homophily in nodes with mixed connections, we define Same-Type Homophily  $Q_s$  and Cross-Type Homophily  $Q_c$ . The representations of target nodes  $\mu_{O_0}$  and  $\mu_{O_1}$  are derived as follows:

$$\begin{aligned} \mu_{O_0} &= \mathbb{E} \left( \mathbf{W} \sum_{j \in \mathcal{N}_r(v_i)} \frac{1}{|\mathcal{N}_r(v_i)|} \mathbf{X}^{(j)} \right) \\ &= \mathbf{W} (Q_s \mu_{\mathbf{X}_0} + (1 - Q_s) \mu_{\mathbf{X}_1} + Q_c \mu_{\mathbf{X}_0} + (1 - Q_c) \mu_{\mathbf{X}_1}) \\ &= \mathbf{W} ((Q_s + Q_c) \mu_{\mathbf{X}_0} + (2 - Q_s - Q_c) \mu_{\mathbf{X}_1}) \end{aligned} \quad (15)$$

$$\begin{aligned} \mu_{O_1} &= \mathbb{E} \left( \mathbf{W} \sum_{j \in \mathcal{N}_r(v_i)} \frac{1}{|\mathcal{N}_r(v_i)|} \mathbf{X}^{(j)} \right) \\ &= \mathbf{W} (Q_s \mu_{\mathbf{X}_1} + (1 - Q_s) \mu_{\mathbf{X}_0} + Q_c \mu_{\mathbf{X}_1} + (1 - Q_c) \mu_{\mathbf{X}_0}) \\ &= \mathbf{W} ((Q_s + Q_c) \mu_{\mathbf{X}_1} + (2 - Q_s - Q_c) \mu_{\mathbf{X}_0}) \end{aligned} \quad (16)$$

The inter-class distance  $M_{0,1}$  can be computed as:

$$\begin{aligned} M_{0,1}^2 &= \|\mu_{O_0} - \mu_{O_1}\|^2 \\ &= \|\mathbf{W} ((2Q_s + 2Q_c - 2) \mu_{\mathbf{X}_0}) + \mathbf{W} ((2 - 2Q_s - 2Q_c) \mu_{\mathbf{X}_1})\|^2 \\ &= \|(2Q_s + 2Q_c - 2) \mathbf{W} (\mu_{\mathbf{X}_0} - \mu_{\mathbf{X}_1})\|^2 \end{aligned} \quad (17)$$

Applying Jensen's Inequality yields:

$$M_{0,1}^2 \leq (2Q_s + 2Q_c - 2)^2 \cdot \|\mathbf{W} (\mu_{\mathbf{X}_0} - \mu_{\mathbf{X}_1})\|^2 \quad (18)$$

The intra-class variances for classes 0 and 1 are computed as:

$$\begin{aligned} T_0^2 &= \mathbb{E} \left( \langle O_0^{(j)} - \mu_{O_0}, O_0^{(j)} - \mu_{O_0} \rangle \right) \\ &= \mathbb{E} \left( (Q_s + Q_c)^2 \cdot (X_0 - \mu_{X_0})^T \cdot \mathbf{W}^T \mathbf{W} \cdot (X_0 - \mu_{X_0}) \right) \\ &\quad + \mathbb{E} \left( (2 - Q_s - Q_c)^2 \cdot (X_1 - \mu_{X_1})^T \cdot \mathbf{W}^T \mathbf{W} \cdot (X_1 - \mu_{X_1}) \right) \end{aligned} \quad (19)$$

We introduce the substitutions  $F = (Q_s + Q_c) \mathbf{W}$ ,  $G = (2 - Q_s - Q_c) \mathbf{W}$ ,  $\Delta X_0 = X_0 - \mu_{X_0}$ , and  $\Delta X_1 = X_1 - \mu_{X_1}$ , allowing us to rewrite  $T_0^2$  as:

$$T_0^2 = \mathbb{E} ((\Delta X_0)^T \cdot F^T F \cdot \Delta X_0) + \mathbb{E} ((\Delta X_1)^T \cdot G^T G \cdot \Delta X_1) \quad (20)$$

Similarly,  $T_1^2$  becomes:

$$T_1^2 = \mathbb{E} ((\Delta X_0)^T \cdot G^T G \cdot \Delta X_0) + \mathbb{E} ((\Delta X_1)^T \cdot F^T F \cdot \Delta X_1) \quad (21)$$

Utilizing the inequality  $x^T \cdot (F^T F + G^T G) \cdot x \geq x^T \cdot (\frac{1}{2} \cdot (F + G)^T (F + G)) \cdot x$ , where equality holds if  $F = G$  and  $F + G = 2\mathbf{W}$ , we obtain:

$$\begin{aligned} T_0^2 + T_1^2 &\geq \frac{1}{2} \mathbb{E} \left[ \Delta X_0^T \cdot (2\mathbf{W})^T (2\mathbf{W}) \cdot \Delta X_0 \right] \\ &\quad + \frac{1}{2} \mathbb{E} \left[ \Delta X_1^T \cdot (2\mathbf{W})^T (2\mathbf{W}) \cdot \Delta X_1 \right] \end{aligned} \quad (22)$$

Therefore, the lower bound  $C_{\text{lower}}$  of the complexity measure  $C$  can be computed as:

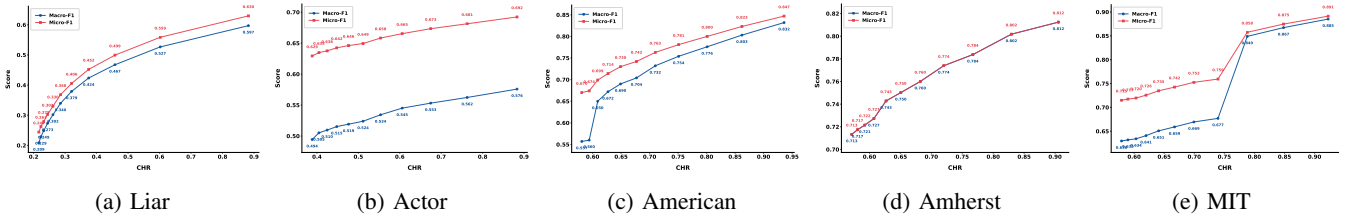


Fig. 4: Relationship between CHR and F1 scores on HGs with varying CHR values.

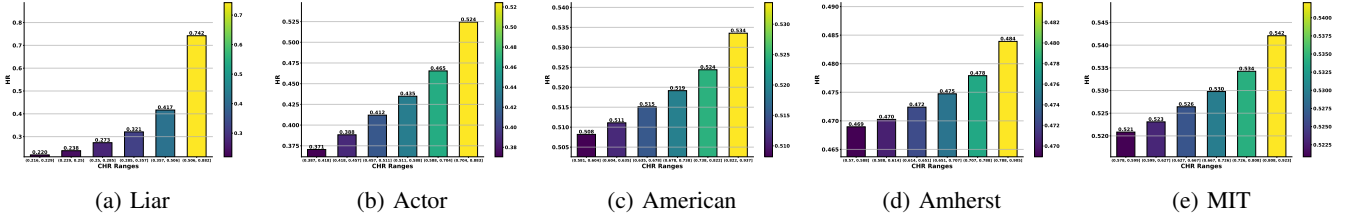


Fig. 5: Relationship between CHR and HR on HGs across different CHR intervals.

$$\begin{aligned}
 C &= \frac{T_0^2 + T_1^2}{M_{0,1}^2} \\
 &\geq 2 \cdot \frac{\mathbb{E}[\Delta X_0^T \cdot \mathbf{W}\mathbf{W}^T \cdot \Delta X_0] + \mathbb{E}[\Delta X_1^T \cdot \mathbf{W}\mathbf{W}^T \cdot \Delta X_1]}{(2Q_s + 2Q_c - 2) \cdot \|\mathbf{W}(\mu_{\mathbf{x}_0} - \mu_{\mathbf{x}_1})\|^2} \quad (23)
 \end{aligned}$$

The components independent of  $Q_c$  in both the numerator and denominator form a positive constant  $C_0$ :

$$C_0 = 2 \cdot \frac{\mathbb{E}[\Delta X_0^T \cdot \mathbf{W}\mathbf{W}^T \cdot \Delta X_0] + \mathbb{E}[\Delta X_1^T \cdot \mathbf{W}\mathbf{W}^T \cdot \Delta X_1]}{\|\mathbf{W}(\mu_{\mathbf{x}_0} - \mu_{\mathbf{x}_1})\|^2} \quad (24)$$

Thus, the lower bound  $C_{\text{lower}}$  becomes:

$$C_{\text{lower}} = \frac{C_0}{(2Q_s + 2Q_c - 2)^2} \quad (25)$$

The partial derivative of  $C_{\text{lower}}$  with respect to  $Q_c$  is:

$$\frac{\partial C_{\text{lower}}}{\partial Q_c} = -\frac{2C_0}{(2Q_s + 2Q_c - 2)^3} \quad (26)$$

As  $Q_c \rightarrow 1$ , the lower bound  $C_{\text{lower}}$  attains its minimum, signifying an optimal state of generalization. This result highlights that increasing cross-type homophily within a heterogeneous graph significantly enhances the generalization capability of HGNNs.  $\square$

### C. Understanding the Impact of CHR

In this subsection, we instantiate the proposed CHR concept and further investigate the relationship between CHR and HGNN performance by constructing HGs with varying CHR values and applying HGNNs.

To investigate this connection, we create HGs with varying CHR values by modifying their structural characteristics. We partition these HGs into training, validation, and test sets at

a consistent ratio and train a unified multi-GCN model. The multi-GCN model applies a projection matrix to map features of different node types in the HG to a common vector space, enabling uniform processing of diverse nodes. Specifically, for each HG, we construct a series of HGs with different CHR values and then evaluate the performance of the HGNN within a specific CHR range. The results presented in Fig. 4, demonstrate a positive correlation between CHR and F1 performance, with multi-GCN performance improving as CHR increases in the target node classification task. This trend confirms that higher CHR values enhance HGNN performance. Meanwhile, as shown in Fig. 5, increasing CHR simultaneously raises the target homophily ratio within HG, which in turn boosts HGNN effectiveness in node classification tasks.

In summary, the Cross-Type Homophily Ratio is a critical metric for assessing cross-type homophily in HGs. By calculating CHR, we can quantify the degree of homophily between different node types. For a given HG, increasing its CHR value can improve the performance of HGNNs in node classification tasks.

## V. UNLEASHING CHR TO BOOST HGNNs

### A. CHR-guided Heterogeneous Graph Pruning

Based on cross-type homophily theory, we propose a pruning method for HGs that focuses on selectively removing cross-type edges with low homophily to enhance information alignment across different node types. By leveraging targeted information propagation and pruning strategies, this approach improves HGNN performance on heterogeneous graph tasks. The overview of CTHGP is depicted in Fig. 6.

The CTHGP framework consists of four processes:

- **Target Information Initialization.** The target information for nodes is derived as follows: known labels are represented in one-hot encoding, while unknown labels are computed using Equation 2. This results in the initial target information matrix  $L \in \mathbb{R}^{N_t \times C}$ , where  $N_t$  is the

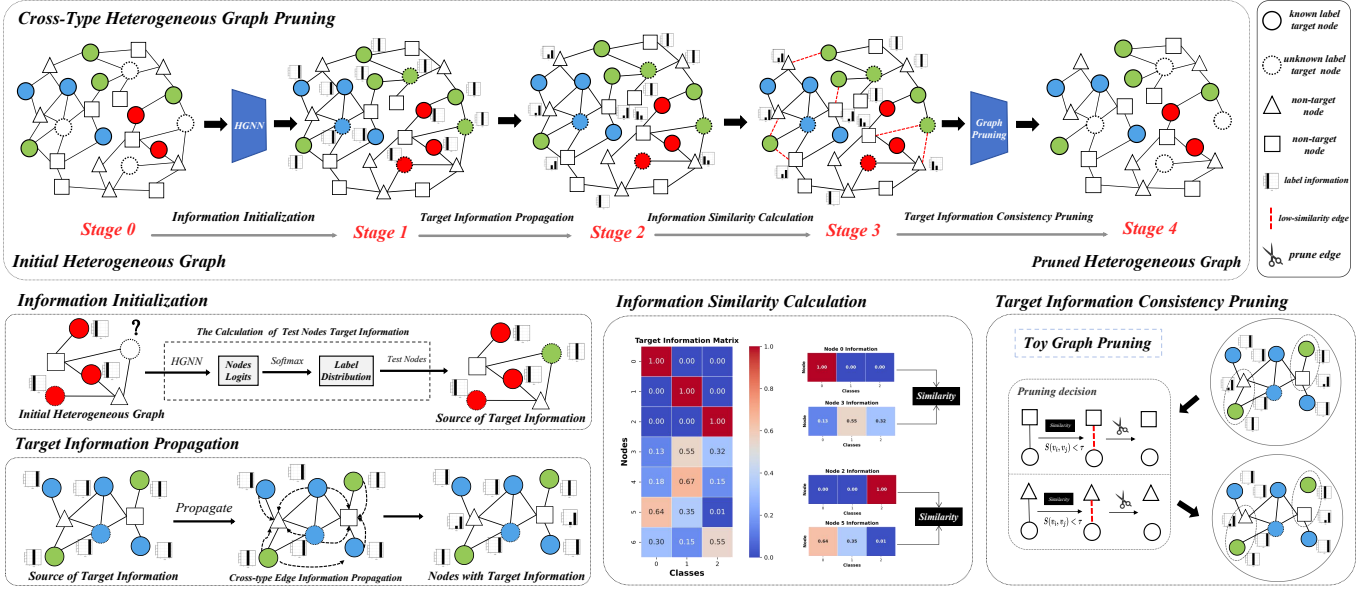


Fig. 6: Overview of the CTHGP Method. The process begins at *Stage 0*, where an HGNN processes the initial heterogeneous graph to assign unknown labels to target nodes, creating a source of target information. At *Stage 1*, this target information is propagated across cross-type edges to non-target nodes. At *Stage 2*, similarity scores are computed for cross-type edges based on the propagated target information. At *Stage 3*, edges with similarity scores below a threshold  $\tau$  are pruned, resulting in a pruned heterogeneous graph at *Stage 4*.

number of target nodes and  $C$  is the number of label categories.

- **Target Information Propagation.** The target information for non-target nodes  $P' \in \mathbb{R}^{N_n \times C}$  is computed using Equations 3 to 5, where  $N_n$  is the number of non-target nodes. Subsequently, the target information matrix  $I \in \mathbb{R}^{N \times C}$ , with  $N = N_t + N_n$  as the total number of nodes, is obtained via Equation 6.
- **Information Similarity Calculation.** This process calculates the similarity of each node based on the definition of CHR and Equation 7. Specifically, in conjunction with graph pruning, the similarity  $\mathcal{S}$  for each node is computed using the target information matrix  $I$  as shown in Equation 27.
- **Target Information Consistency Pruning.** We use graph pruning to remove cross-type edges with low homophily, thereby increasing the CHR of HGs and enhancing information alignment across different node types.

The details of the preceding steps are presented in subsection IV-A. Based on the CHR calculations, we derived the target information matrix  $I$ . A graph pruning strategy is employed to refine the graph structure by assessing node similarity. This strategy is a low-complexity algorithm that effectively reduces the graph’s complexity while simultaneously achieving our goal of enhancing CHR. In the following, we provide a detailed explanation of **Target Information Consistency Pruning**. Specifically, we first establish a formal definition of graph pruning, present a comprehensive analysis of the techniques adopted in our approach, and elucidate how

$I$  is utilized to improve the CHR of HGs.

#### Definition 6. Graph Pruning.

*Graph pruning is defined as a mapping function  $\Gamma : \mathcal{G}(\mathcal{V}, \mathcal{E}) \rightarrow \mathcal{G}'(\mathcal{V}, \mathcal{E}')$ , where  $\mathcal{G} = (\mathcal{V}, \mathcal{E})$  is the original graph with the node set  $\mathcal{V}$  and  $\mathcal{E}$ , and  $\mathcal{G}'(\mathcal{V}, \mathcal{E}')$  is the pruned graph with the node set  $\mathcal{V}$  and the pruned edge set  $\mathcal{E}' \subseteq \mathcal{E}$ . The pruning decision is based on a decision function  $\mathcal{F} : \mathcal{V} \times \mathcal{V} \rightarrow \{0, 1\}$  that determines whether an edge satisfies a given condition. With the decision function, the pruned edge set can be rewritten as  $\mathcal{E}' = \{(v_i, v_j) \in \mathcal{E} \mid \mathcal{F}(v_i, v_j) = 1\}$ .*

Graph pruning is an operation that reduces the number of edges without increasing the complexity of the graph, while preserving the necessary structural and relational information. The decision function can be instantiated in multiple ways. In this work, we instantiate the decision function  $\mathcal{F}$  using a similarity function  $\mathcal{S}$  and a threshold  $\tau$ . The similarity function  $\mathcal{S} : \mathcal{V} \times \mathcal{V} \rightarrow [0, 1]$  assigns a similarity score to each edge, while the pruning threshold  $\tau \in [0, 1]$  determines whether an edge is retained. Specifically,  $\mathcal{F}(v_i, v_j)$  is defined as  $\mathcal{F}(v_i, v_j) = 1$  if  $\mathcal{S}(v_i, v_j) \geq \tau$ , and  $\mathcal{F}(v_i, v_j) = 0$  otherwise. The pruning function simplifies the edge set of a graph  $\mathcal{G}$  by computing edge similarity scores with a similarity function  $\mathcal{S}$  and removing edges with scores below a threshold  $\tau$ , where  $\tau$  serves as a hyperparameter to control the pruning intensity and flexibility. Specifically, for an edge  $e_{ij} \in \mathcal{E}_{\text{target-non}}$  connecting a target-type node  $v_i$  with a non-target node  $v_j$ , the similarity



of target information is defined as:

$$\mathcal{S}(v_i, v_j) = I(v_i)^\top I(v_j) \quad (27)$$

Then, a threshold  $\tau$  is set for pruning, and edges are removed if their similarity  $\mathcal{S}(v_i, v_j)$  falls below  $\tau$ . Consequently, the pruned graph structure  $\mathcal{G}_{\text{pruning}}$  is defined as:

$$\mathcal{G}_{\text{pruning}} = (\mathcal{V}, \mathcal{E}_{\text{pruning}}) \quad (28)$$

where  $\mathcal{E}_{\text{pruning}}$  consists of edges that meet the pruning criterion:

$$\mathcal{E}_{\text{pruning}} = \{(v_i, v_j) \mid \mathcal{S}(v_i, v_j) \geq \tau\} \quad (29)$$

The resulting pruned graph structure is then used as input for heterogeneous graph learning tasks. By selectively removing edges with similarity less than  $\tau$ , we enhance the CHR value of the initial HG while reducing the graph’s complexity. The pruned HGs are then directly fed into HGNNs for node classification tasks on HGs.

### B. Complexity Analysis

The time complexity of CTHGP can be analyzed across three primary stages. First, during the Information Propagation and Initialization phase, label information for target-type nodes is generated through one-hot encoding and predictions using an HGNN, with complexity  $O(N_t C + N_t F^2 L)$ , where  $N_t$  denotes the number of target nodes,  $C$  the number of classes,  $F$  the hidden units in the HGNN, and  $L$  the network depth. In the Propagation of Target Information phase, target information is diffused across the graph using cross-type adjacency and propagation matrices, with complexity  $O(N_n N_t C)$ , where  $N_n$  represents the number of non-target nodes. This phase’s complexity primarily arises from matrix multiplication operations. Finally, during the Target Information Consistency Pruning stage, similarity calculations between target and non-target nodes are performed, with complexity  $O(N_t N_n C)$ . The complexity for pruning decisions is proportional to the edge count  $|\mathcal{E}|$ , yielding  $O(|\mathcal{E}|)$ . Hence, the total time complexity is  $O(N_t C + N_t F^2 L + N_n N_t C + |\mathcal{E}|)$ . The relatively small values of  $C$ ,  $L$ , and  $F$  mean they contribute minimally to computational load.

**Core Computation Bottleneck Analysis.** The complexity in the information propagation phase  $O(N_n N_t C)$  and similarity computation  $O(N_t N_n C)$  represent the primary computational bottlenecks. While  $N_n N_t$  suggests quadratic growth, in HGs,  $N_n$  typically exceeds  $N_t$ . With  $C$  constant, complexity growth remains controlled, leading to a linear increase as node counts rise. Overall, the algorithm’s complexity is primarily driven by information propagation and similarity computation, yielding a complexity of  $O(N_n N_t C)$  and demonstrating strong scalability.

## VI. EXPERIMENTAL EVALUATION

### A. Experimental Setup

**Datasets.** We evaluated our method on five real-world heterogeneous graph datasets. Details of these datasets are shown in Table I.

TABLE I: Statistics of datasets.

Dataset	#Nodes	#Node Types	#Edges	#Edge Types	Target	#Classes
American	9,473	7	465,557	13	person	2
Liar	14,395	4	45,358	6	news	6
Actor	16,255	3	76,118	18	star	7
Amherst	3,422	7	190,277	13	person	2
MIT	9,274	7	532,102	13	person	2

- **Liar** [58] is a heterogeneous graph network developed for Fake News Detection. It contains four distinct node types and six edge types, with the task of predicting the category of news nodes.
- **American, Amherst, and MIT** are three datasets selected from the FB100 collection, representing heterogeneous networks of Facebook “friendship” structures across 100 American colleges and universities, captured at a single point in time [59]. Specifically, we used datasets from MIT (8th), Amherst (41st), and American (75th) in the FB100 collection, each containing seven node types and thirteen edge types. The task for these datasets is to classify the gender of person nodes.
- **Actor** [60] is a film-related heterogeneous network extracted from Wikipedia. It contains three node types and eighteen edge types, with the task of predicting the category of actor nodes.

**Baseline Methods.** We evaluated our method using seven graph neural networks, which include four homogeneous GNNs (GCN, GAT, H2GCN, LINKX) and three heterogeneous GNNs (RGCN, SHGN, HINormer). Additionally, we compared our method’s performance in graph structure learning with four established methods.

- **GCN** [61]: A semi-supervised graph convolutional network that learns node embeddings by aggregating information from neighboring nodes.
- **GAT** [62]: Employs attention mechanisms to selectively aggregate features from neighboring nodes.
- **H2GCN** [9]: Separates ego-embedding and neighbor-embedding, utilizes higher-order neighborhoods, and fuses intermediate representations to enhance performance in graphs with heterophily.
- **LINKX** [63]: Decouples structural transformations from feature transformations, combining them to achieve superior performance on heterophily graphs.
- **RGCN** [24]: Assigns distinct parameters to different relations, aggregating neighboring representations based on their specific types.
- **SHGN** [18]: Computes attention scores for different relations and normalizes the outputs using the L2-norm.
- **HINormer** [28]: Utilizes a wide-range aggregation mechanism for node representation learning, employing both a local structure encoder and a heterogeneous relation encoder.

**Graph Structure Learning Baselines.** We further evaluated our method in comparison with four prominent graph structure learning approaches:

- **LDS** [64] is a graph structure learning method that optimizes graph structures through bilevel optimization to enhance task performance.
- **IDGL** [42] is a graph structure learning method that iteratively refines graph topology based on task performance, continuously updating the learned structure.
- **HGSL** [49] is a heterogeneous graph structure learning method that integrates attribute, meta-path, and structural information to guide relation learning in HGs.
- **HDHGR** [13] is a homophily-oriented graph rewiring approach that modifies the graph structure to boost the performance of HGNNs.

**Implementation Setup.** In the baseline for GNNs on homogeneous graphs, we map the features of different node types in the HGs to the same dimensional space, treating the HG as a homogeneous graph. We refer to this modified GCN with feature mapping as multi-GCN, and all GCNs used in this paper follow this setting. For HGNNs on HGs, We implement the models based on the configurations specified in their previous papers. For graph structure learning methods on homogeneous graphs, we disregard the node and edge types of the HG and treat it as a homogeneous input. The methods on HGs are implemented using the parameter settings provided in their corresponding papers. The datasets are split into training, validation, and testing sets with a 0.6/0.2/0.2 ratio. All models are trained for 400 epochs using the Adam optimizer, with a learning rate of  $5e-4$  and a weight decay of  $1e-4$ . The pruning threshold is searched within the range  $[0, 1]$  at intervals of 0.05 or 0.1, and the results are averaged over five random seeds. All experiments are conducted on two 32GB V100 GPUs.

**Evaluation Metrics.** We performed node classification tasks on HGNNs, using Macro-F1 and Micro-F1 scores as evaluation metrics. For each HGNN, we tested the model on both the original and pruned HGs to evaluate the performance improvement introduced by our pruning method. To further assess the generalizability of our method across different datasets, we calculated the average relative improvement (ARI) for all models on each dataset as an additional metric.

$$\text{ARI} = \frac{1}{|\mathcal{M}|} \sum_{m_i \in \mathcal{M}} \left( \frac{\text{ACC}(m_i(\hat{\mathcal{G}})) - \text{ACC}(m_i(\mathcal{G}))}{\text{ACC}(m_i(\mathcal{G}))} \right) \quad (30)$$

where  $\mathcal{M}$  represents the set of evaluated models,  $\hat{\mathcal{G}}$  is the pruned HG, and  $\mathcal{G}$  is the original HG. All experiments were repeated five times, and we report the mean results and standard deviations.

## B. Main Results Analysis

We conducted node classification experiments on HGs to evaluate the effectiveness of our method by comparing the performance of HGNNs before and after applying pruning. The results, presented in Table II., show that our pruning method can be applied to all seven HGNN models used as backbones in the baseline and leads to significant improvements across all five heterogeneous graph datasets. This demonstrates the broad

applicability and effectiveness of our method. The Macro-F1 metric, which equally prioritizes each class regardless of its instance frequency, demonstrates a significantly higher improvement relative to Micro-F1, which scales performance based on instance counts. This marked enhancement in Macro-F1 suggests that our proposed method is especially adept at bolstering classification efficacy within long-tail categories. Thus, CTHGP is further capable of tackling a critical challenge in imbalanced data distributions.

As shown in In Fig. 7, we analyze changes in CHR before and after pruning. Comparison results reveal that pruning enhances the CHR of HGs, indicating that the CTHGP method effectively increases the cross-type homophily level within HGs, thereby boosting the overall performance of HGNNs on these datasets. When analyzing individual datasets, we found that the CTHGP method achieved the highest ARI on the Liar dataset. The initial CHR of Liar was much lower than that of the other datasets, at only 21.66%, indicating a high degree of heterophily in the cross-type edges. This further suggests that the CTHGP method excels in HGs with low initial homophily.

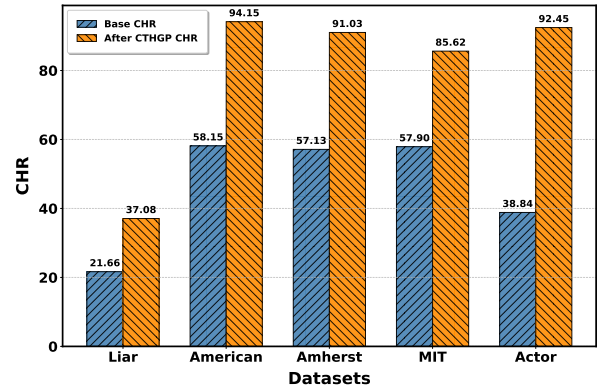
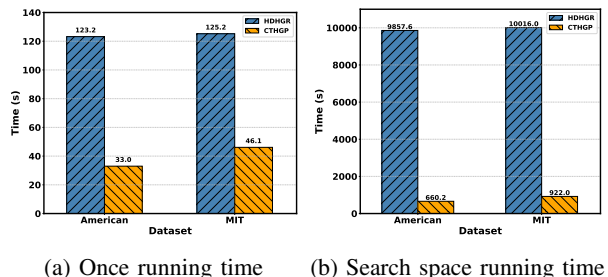


Fig. 7: CHR comparison before and after CTHGP. *Base CHR* represents the CHR value of the HG before CTHGP, while *After CTHGP CHR* denotes the CHR value of the HG after applying CTHGP method.



(a) Once running time (b) Search space running time

Fig. 8: Running time comparison between CTHGP and HDHGR. (a) shows once running time of the method with 400 epochs, while (b) presents best search space running time of the method with 400 epochs.

TABLE II: Node classification results on HG datasets. The bold numbers indicate that our method improves the base model.

Method	/	Liar		Actor		American		Amherst		MIT	
		Macro-F1	Micro-F1	Macro-F1	Micro-F1	Macro-F1	Micro-F1	Macro-F1	Micro-F1	Macro-F1	Micro-F1
GCN	origin	20.75 ± 1.40	23.40 ± 1.97	48.78 ± 1.30	61.85 ± 1.41	57.30 ± 7.24	66.86 ± 3.35	71.33 ± 1.77	71.34 ± 1.78	65.40 ± 8.02	70.93 ± 3.76
	CTHGP	<b>24.07 ± 1.73</b>	<b>25.00 ± 0.52</b>	<b>52.57 ± 1.21</b>	<b>63.20 ± 1.13</b>	<b>68.77 ± 0.99</b>	<b>69.83 ± 1.01</b>	<b>73.78 ± 0.38</b>	<b>73.79 ± 0.38</b>	<b>75.04 ± 0.24</b>	<b>77.31 ± 0.22</b>
GAT	origin	23.81 ± 1.66	24.43 ± 1.98	45.65 ± 1.03	61.26 ± 1.02	64.19 ± 0.30	68.05 ± 0.37	71.73 ± 1.12	71.74 ± 1.26	73.99 ± 1.42	75.16 ± 1.26
	CTHGP	<b>24.52 ± 0.22</b>	<b>24.74 ± 0.25</b>	<b>50.81 ± 0.65</b>	<b>62.01 ± 0.92</b>	<b>73.66 ± 1.16</b>	<b>76.39 ± 1.08</b>	<b>74.27 ± 0.36</b>	<b>74.28 ± 0.37</b>	<b>77.50 ± 1.51</b>	<b>78.60 ± 1.31</b>
H2GCN	origin	19.84 ± 0.31	22.00 ± 1.60	51.42 ± 1.21	63.13 ± 1.34	75.73 ± 0.29	77.33 ± 0.49	80.74 ± 0.37	80.75 ± 0.31	78.69 ± 2.13	79.48 ± 1.91
	CTHGP	<b>22.03 ± 1.19</b>	<b>23.19 ± 1.36</b>	<b>53.20 ± 1.39</b>	<b>63.49 ± 1.62</b>	<b>76.52 ± 0.21</b>	<b>78.33 ± 0.56</b>	<b>81.89 ± 1.85</b>	<b>81.90 ± 1.80</b>	<b>81.55 ± 1.16</b>	<b>82.55 ± 1.10</b>
LINKX	origin	17.26 ± 1.43	19.04 ± 2.74	50.60 ± 1.02	55.83 ± 1.12	74.47 ± 0.45	74.81 ± 0.49	81.88 ± 1.99	81.88 ± 1.98	77.06 ± 2.07	77.28 ± 2.20
	CTHGP	<b>19.47 ± 2.12</b>	<b>20.13 ± 2.05</b>	<b>52.81 ± 1.37</b>	<b>57.77 ± 0.98</b>	<b>77.60 ± 0.56</b>	<b>79.27 ± 0.75</b>	<b>83.12 ± 1.64</b>	<b>83.13 ± 1.63</b>	<b>80.40 ± 0.39</b>	<b>80.91 ± 0.40</b>
RGCN	origin	17.71 ± 0.53	22.58 ± 2.10	65.62 ± 1.34	78.31 ± 1.01	52.57 ± 2.77	64.03 ± 1.12	60.74 ± 3.43	60.93 ± 3.22	67.17 ± 3.12	69.24 ± 2.85
	CTHGP	<b>20.34 ± 1.13</b>	<b>22.95 ± 0.95</b>	<b>71.36 ± 1.41</b>	<b>82.48 ± 0.92</b>	<b>55.22 ± 1.90</b>	<b>63.65 ± 0.52</b>	<b>62.72 ± 2.82</b>	<b>62.90 ± 2.65</b>	<b>69.08 ± 2.05</b>	<b>70.79 ± 2.20</b>
SHGN	origin	21.31 ± 1.44	24.35 ± 1.82	70.63 ± 0.93	78.95 ± 1.18	75.17 ± 3.65	77.22 ± 2.83	79.77 ± 1.69	79.85 ± 1.72	77.91 ± 2.22	79.05 ± 1.99
	CTHGP	<b>24.42 ± 0.06</b>	<b>25.66 ± 0.51</b>	<b>73.11 ± 0.85</b>	<b>81.29 ± 0.74</b>	<b>78.15 ± 0.59</b>	<b>79.55 ± 0.49</b>	<b>82.88 ± 3.56</b>	<b>82.81 ± 3.50</b>	<b>81.12 ± 0.41</b>	<b>82.06 ± 0.56</b>
HINormer	origin	20.29 ± 1.13	23.18 ± 1.70	47.72 ± 1.34	63.05 ± 0.59	66.57 ± 1.63	70.02 ± 1.54	72.09 ± 1.44	72.15 ± 1.50	73.15 ± 2.26	74.48 ± 2.46
	CTHGP	<b>24.60 ± 0.39</b>	<b>25.10 ± 0.35</b>	<b>52.87 ± 1.76</b>	<b>65.71 ± 0.62</b>	<b>75.62 ± 1.10</b>	<b>77.53 ± 1.04</b>	<b>80.90 ± 2.43</b>	<b>80.92 ± 2.42</b>	<b>77.26 ± 1.28</b>	<b>78.54 ± 1.05</b>
ARI	/	<b>13.36%↑</b>	<b>4.93%↑</b>	<b>7.14%↑</b>	<b>2.85%↑</b>	<b>8.95%↑</b>	<b>5.30%↑</b>	<b>4.18%↑</b>	<b>4.15%↑</b>	<b>5.72%↑</b>	<b>4.80%↑</b>

TABLE III: Performance comparison of graph structure learning methods.

Method	Liar		American		MIT	
	Macro-F1	Micro-F1	Macro-F1	Micro-F1	Macro-F1	Micro-F1
Base Model	20.75 ± 1.40	23.40 ± 1.97	57.30 ± 7.24	66.86 ± 3.35	65.40 ± 8.02	70.93 ± 3.76
LDS	20.95 ± 1.87	22.92 ± 1.70	58.42 ± 5.98	66.92 ± 3.44	67.67 ± 2.25	71.00 ± 2.37
IDGL	21.99 ± 1.71	23.02 ± 1.92	58.85 ± 4.34	67.10 ± 2.20	68.88 ± 3.27	72.74 ± 3.21
HGSL	21.01 ± 0.89	23.10 ± 1.41	58.93 ± 2.11	67.01 ± 1.87	68.32 ± 2.69	72.15 ± 2.12
HDHGR	23.01 ± 0.63	24.19 ± 0.81	65.72 ± 2.06	67.92 ± 0.94	73.91 ± 1.72	74.65 ± 1.06
CTHGP	<b>24.07 ± 1.73</b>	<b>25.00 ± 0.52</b>	<b>68.77 ± 0.99</b>	<b>69.83 ± 1.01</b>	<b>75.04 ± 0.24</b>	<b>77.31 ± 0.22</b>

TABLE IV: Ablation study results on HG datasets.

Method	Liar		Actor		American		Amherst		MIT	
	Macro-F1	Micro-F1	Macro-F1	Micro-F1	Macro-F1	Micro-F1	Macro-F1	Micro-F1	Macro-F1	Micro-F1
Base Model	20.75 ± 1.40	23.40 ± 1.97	48.78 ± 1.30	61.85 ± 1.41	57.30 ± 7.24	66.86 ± 3.35	71.33 ± 1.77	71.34 ± 1.78	65.40 ± 8.02	70.93 ± 3.76
RandDropEdge	19.30 ± 1.48	22.68 ± 1.30	48.34 ± 1.32	61.93 ± 1.48	56.12 ± 7.39	66.03 ± 3.63	70.54 ± 1.47	70.51 ± 1.48	64.53 ± 7.36	69.85 ± 3.31
CTHGP	<b>24.07 ± 1.73</b>	<b>25.00 ± 0.52</b>	<b>52.57 ± 1.21</b>	<b>63.20 ± 1.13</b>	<b>68.77 ± 0.99</b>	<b>69.83 ± 1.01</b>	<b>73.78 ± 0.38</b>	<b>73.79 ± 0.38</b>	<b>75.04 ± 0.24</b>	<b>77.31 ± 0.22</b>

### C. Comparison with Graph Structure Learning Methods

We compare CTHGP with four graph structure learning methods, using multi-GCN, an extension of GCN that maps node features from various categories into a unified feature space. As shown in Table III, our method consistently outperforms the others, demonstrating its effectiveness.

To further compare with the second-best method, HDHGR, we analyzed runtime efficiency and design complexity. As illustrated in Fig. 8, our approach significantly reduces runtime for a single model execution compared to HDHGR. Incorporating our complexity analysis alongside the analysis presented in HDHGR, this demonstrates that our method offers superior

efficiency and scalability for graphs. Specifically, CTHGP requires only a single hyperparameter tuning for the pruning threshold, typically optimized within the range of [0, 1] in intervals of 0.1. For higher precision, intervals of 0.05 can be used. In contrast, the HDHGR method involves an extensive hyperparameter search over three variables, requiring up to 80 searches for optimal results. Our method outperforms HDHGR by several times in single-run runtime and is more than ten times faster than HDHGR in search space runtime.

HDHGR employs a complex meta-path-based strategy with same-type edges and exhibits high time complexity. Meanwhile, HDHGR requires careful adjustment of multiple param-

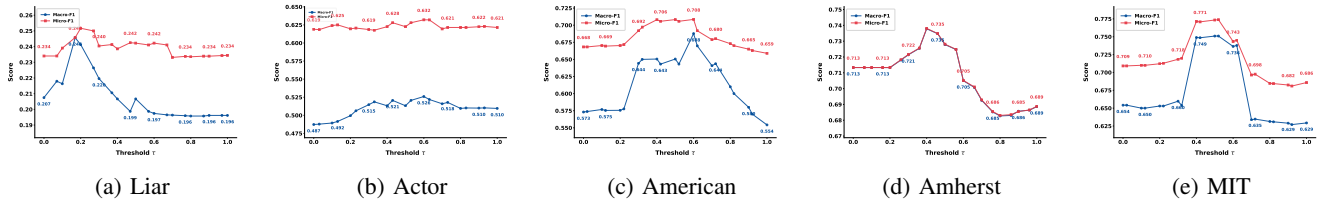


Fig. 9: Hyper-parameter study of pruning threshold  $\tau$  and F1.

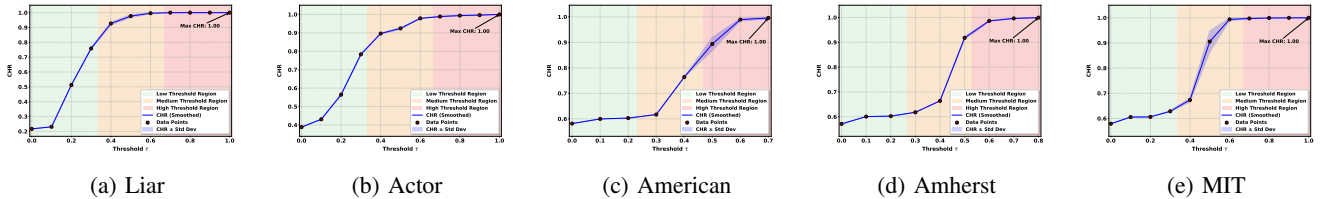


Fig. 10: Hyper-parameter study of pruning threshold  $\tau$  and CHR.

eters, resulting in significant time consumption and limiting its utility in real-world applications. Our method begins by analyzing cross-type edges and adopts a simple yet highly effective edge pruning strategy, which efficiently refines the graph structure with lower computational complexity. This approach significantly enhances HGNNs performance without increasing graph complexity, thereby facilitating its efficient use in practical applications. This result emphasizes the effectiveness of our approach and highlights the potential of focusing on cross-type edges in HGs as a compelling avenue for future research.

#### D. Ablation Study

We conduct an ablation study to evaluate the effectiveness of target information pruning, using multi-GCN as the base model. Table IV presents the experimental results. We employ a random graph structure transformation technique, RandDropEdge, which removes edges from the original graph with a probability of 50%, and tested the performance of GCN. We observed that random pruning at this probability led to performance declines across models, while our pruning method resulted in substantial improvements. This finding demonstrates the effectiveness of our target information pruning approach.

#### E. Hyper-parameter Study

**Pruning Threshold  $\tau$  and Model Performance.** As shown in Fig. 9, we observe an approximately unimodal relationship between the pruning threshold  $\tau$  and model performance. The best performance is typically achieved with pruning thresholds  $\tau$  in the range of 0.3 to 0.6. Both low and high thresholds yield suboptimal performance: with a low threshold, heterophilic edges are insufficiently pruned, limiting the effectiveness of the pruning algorithm. Conversely, a high threshold imposes strict requirements on edge retention, retaining only a small set of high-homophily edges, which can diminish HGNNs performance.

**Pruning Threshold  $\tau$  and CHR.** We vary the value of each pruning threshold  $\tau$  and record the CHR of the pruned HG, as shown in Fig. 10. We observe that as the pruning threshold  $\tau$  increases, CHR also rises, indicating a growing proportion of homophilous edges among cross-type edges in the pruned dataset. However, model performance initially improves with increasing pruning threshold  $\tau$  and subsequently declines, unlike CHR, which continues to increase. This divergence occurs because, beyond a certain threshold, the pruning process begins to eliminate many cross-type edges that exhibit homophily, retaining only a few with very high homophily. This can result in an overall decrease in the graph’s Extended Target Homophily Ratio. Consequently, a low pruning threshold  $\tau$  does not achieve sufficient pruning, while an excessively high threshold removes too many homophilous cross-type edges. A mid-range pruning threshold  $\tau$  generally yields optimal model performance.

## VII. CONCLUSION AND FUTURE WORK

This study introduces CHR, a novel metric to quantify cross-type homophily in HGs, marking the first exploration of cross-type edges in this field. We establish its theoretical foundations, validate it empirically, and propose CTHGP, a pruning method that enhances CHR and improves HGNNs performance. As a versatile and efficient plug-in compatible with various HGNN architectures, CTHGP demonstrates its effectiveness in improving CHR and node classification performance in experiments.

The concept of cross-type homophily proposed in this work is flexible and broad. We instantiated CHR using target node labels but noted that it can also utilize other information, such as features. Future research may explore enhancing CHR by adding homophilous cross-type edges, though this approach is less efficient than pruning. Pruning remains a more effective method for simplifying graph structures and improving both computational efficiency and HGNN performance.

## REFERENCES

- [1] G. Ertug, J. Brennecke, B. Kovács, and T. Zou, “What does homophily do? a review of the consequences of homophily,” *Academy of Management Annals*, vol. 16, no. 1, pp. 38–69, 2022.
- [2] G. Kossinets and D. J. Watts, “Origins of homophily in an evolving social network,” *American journal of sociology*, vol. 115, no. 2, pp. 405–450, 2009.
- [3] Q. Sun, K. Wang, W. Zhang, P. Cheng, and X. Lin, “Interdependence-adaptive mutual information maximization for graph contrastive learning,” *IEEE Transactions on Knowledge and Data Engineering*, 2024.
- [4] Q. Sun, W. Zhang, and X. Lin, “Progressive hard negative masking: From global uniformity to local tolerance,” *IEEE Transactions on Knowledge and Data Engineering*, vol. 35, no. 12, pp. 12932–12943, 2023.
- [5] M. McPherson, L. Smith-Lovin, and J. M. Cook, “Birds of a feather: Homophily in social networks,” *Annual review of sociology*, vol. 27, no. 1, pp. 415–444, 2001.
- [6] H. Pei, B. Wei, K. C.-C. Chang, Y. Lei, and B. Yang, “Geom-gcn: Geometric graph convolutional networks,” *arXiv preprint arXiv:2002.05287*, 2020.
- [7] C. Lozares, J. M. Verd, I. Cruz, and O. Barranco, “Homophily and heterophily in personal networks. from mutual acquaintance to relationship intensity,” *Quality & Quantity*, vol. 48, pp. 2657–2670, 2014.
- [8] S. Luan, M. Zhao, C. Hua, X.-W. Chang, and D. Precup, “Complete the missing half: Augmenting aggregation filtering with diversification for graph convolutional networks,” *arXiv preprint arXiv:2008.08844*, 2020.
- [9] J. Zhu, Y. Yan, L. Zhao, M. Heimann, L. Akoglu, and D. Koutra, “Beyond homophily in graph neural networks: Current limitations and effective designs,” *Advances in neural information processing systems*, vol. 33, pp. 7793–7804, 2020.
- [10] S. Luan, C. Hua, Q. Lu, L. Ma, L. Wu, X. Wang, M. Xu, X.-W. Chang, D. Precup, R. Ying *et al.*, “The heterophilic graph learning handbook: Benchmarks, models, theoretical analysis, applications and challenges,” *arXiv preprint arXiv:2407.09618*, 2024.
- [11] X. Zheng, Y. Wang, Y. Liu, M. Li, M. Zhang, D. Jin, P. S. Yu, and S. Pan, “Graph neural networks for graphs with heterophily: A survey,” *arXiv preprint arXiv:2202.07082*, 2022.
- [12] X. Wang, D. Bo, C. Shi, S. Fan, Y. Ye, and S. Y. Philip, “A survey on heterogeneous graph embedding: methods, techniques, applications and sources,” *IEEE Transactions on Big Data*, vol. 9, no. 2, pp. 415–436, 2022.
- [13] J. Guo, L. Du, W. Bi, Q. Fu, X. Ma, X. Chen, S. Han, D. Zhang, and Y. Zhang, “Homophily-oriented heterogeneous graph rewiring,” in *Proceedings of the ACM Web Conference 2023*, 2023, pp. 511–522.
- [14] J. Li, Z. Wei, J. Dan, J. Zhou, Y. Zhu, R. Wu, B. Wang, Z. Zhen, C. Meng, H. Jin *et al.*, “Hetero<sup>2</sup>net: Heterophily-aware representation learning on heterogeneous graphs,” *arXiv preprint arXiv:2310.11664*, 2023.
- [15] J. Zhou, G. Cui, S. Hu, Z. Zhang, C. Yang, Z. Liu, L. Wang, C. Li, and M. Sun, “Graph neural networks: A review of methods and applications,” *AI open*, vol. 1, pp. 57–81, 2020.
- [16] Y. Dong, N. V. Chawla, and A. Swami, “metapath2vec: Scalable representation learning for heterogeneous networks,” in *Proceedings of the 23rd ACM SIGKDD international conference on knowledge discovery and data mining*, 2017, pp. 135–144.
- [17] Y. Zhao, Y. Sun, Y. Huang, L. Li, and H. Dong, “Link prediction in heterogeneous networks based on metapath projection and aggregation,” *Expert Systems with Applications*, vol. 227, p. 120325, 2023.
- [18] Q. Lv, M. Ding, Q. Liu, Y. Chen, W. Feng, S. He, C. Zhou, J. Jiang, Y. Dong, and J. Tang, “Are we really making much progress? revisiting, benchmarking and refining heterogeneous graph neural networks,” in *Proceedings of the 27th ACM SIGKDD conference on knowledge discovery & data mining*, 2021, pp. 1150–1160.
- [19] Z. Wang, D. Yu, Q. Li, S. Shen, and S. Yao, “Sr-hgn: Semantic-and relation-aware heterogeneous graph neural network,” *Expert Systems with Applications*, vol. 224, p. 119982, 2023.
- [20] X. Wang, H. Ji, C. Shi, B. Wang, Y. Ye, P. Cui, and P. S. Yu, “Heterogeneous graph attention network,” in *The world wide web conference*, 2019, pp. 2022–2032.
- [21] X. Fu, J. Zhang, Z. Meng, and I. King, “Magnn: Metapath aggregated graph neural network for heterogeneous graph embedding,” in *Proceedings of the web conference 2020*, 2020, pp. 2331–2341.
- [22] S. Yun, M. Jeong, R. Kim, J. Kang, and H. J. Kim, “Graph transformer networks,” *Advances in neural information processing systems*, vol. 32, 2019.
- [23] Y. Chang, C. Chen, W. Hu, Z. Zheng, X. Zhou, and S. Chen, “Megnn: Meta-path extracted graph neural network for heterogeneous graph representation learning,” *Knowledge-Based Systems*, vol. 235, p. 107611, 2022.
- [24] M. Schlichtkrull, T. N. Kipf, P. Bloem, R. Van Den Berg, I. Titov, and M. Welling, “Modeling relational data with graph convolutional networks,” in *The semantic web: 15th international conference, ESWC 2018, Heraklion, Crete, Greece, June 3–7, 2018, proceedings 15*. Springer, 2018, pp. 593–607.
- [25] H. Hong, H. Guo, Y. Lin, X. Yang, Z. Li, and J. Ye, “An attention-based graph neural network for heterogeneous structural learning,” in *Proceedings of the AAAI conference on artificial intelligence*, vol. 34, no. 04, 2020, pp. 4132–4139.
- [26] Z. Hu, Y. Dong, K. Wang, and Y. Sun, “Heterogeneous graph transformer,” in *Proceedings of the web conference 2020*, 2020, pp. 2704–2710.
- [27] C. Zhang, D. Song, C. Huang, A. Swami, and N. V. Chawla, “Heterogeneous graph neural network,” in *Proceedings of the 25th ACM SIGKDD international conference on knowledge discovery & data mining*, 2019, pp. 793–803.
- [28] Q. Mao, Z. Liu, C. Liu, and J. Sun, “Hinormer: Representation learning on heterogeneous information networks with graph transformer,” in *Proceedings of the ACM Web Conference 2023*, 2023, pp. 599–610.
- [29] S. Brody, U. Alon, and E. Yahav, “How attentive are graph attention networks?” *arXiv preprint arXiv:2105.14491*, 2021.
- [30] D. Bo, X. Wang, C. Shi, and H. Shen, “Beyond low-frequency information in graph convolutional networks,” in *Proceedings of the AAAI conference on artificial intelligence*, vol. 35, no. 5, 2021, pp. 3950–3957.
- [31] S. Luan, C. Hua, Q. Lu, J. Zhu, M. Zhao, S. Zhang, X.-W. Chang, and D. Precup, “Revisiting heterophily for graph neural networks,” *Advances in neural information processing systems*, vol. 35, pp. 1362–1375, 2022.
- [32] E. Chien, J. Peng, P. Li, and O. Milenkovic, “Adaptive universal generalized pagerank graph neural network,” *arXiv preprint arXiv:2006.07988*, 2020.
- [33] J. Chen, Y. Wang, C. Bodnar, R. Ying, P. Lio, and Y. G. Wang, “Dirichlet energy enhancement of graph neural networks by framelet augmentation,” *arXiv preprint arXiv:2311.05767*, 2023.
- [34] Y. Yan, M. Hashemi, K. Swersky, Y. Yang, and D. Koutra, “Two sides of the same coin: Heterophily and oversmoothing in graph convolutional neural networks,” in *2022 IEEE International Conference on Data Mining (ICDM)*. IEEE, 2022, pp. 1287–1292.
- [35] L. Du, X. Shi, Q. Fu, X. Ma, H. Liu, S. Han, and D. Zhang, “Gbk-gnn: Gated bi-kernel graph neural networks for modeling both homophily and heterophily,” in *Proceedings of the ACM Web Conference 2022*, 2022, pp. 1550–1558.
- [36] D. Jin, Z. Yu, C. Huo, R. Wang, X. Wang, D. He, and J. Han, “Universal graph convolutional networks,” *Advances in Neural Information Processing Systems*, vol. 34, pp. 10654–10664, 2021.
- [37] X. Li, R. Zhu, Y. Cheng, C. Shan, S. Luo, D. Li, and W. Qian, “Finding global homophily in graph neural networks when meeting heterophily,” in *International Conference on Machine Learning*. PMLR, 2022, pp. 13242–13256.
- [38] H. Ahn, Y. Yang, Q. Gan, T. Moon, and D. P. Wipf, “Descent steps of a relation-aware energy produce heterogeneous graph neural networks,” *Advances in Neural Information Processing Systems*, vol. 35, pp. 38436–38448, 2022.
- [39] D. Deng, F. Bai, Y. Tang, S. Zhou, C. Shahabi, and L. Zhu, “Label propagation on k-partite graphs with heterophily,” *IEEE Transactions on Knowledge and Data Engineering*, vol. 33, no. 3, pp. 1064–1077, 2019.
- [40] T. Xiong, C. Qiu, and P. Zhang, “How ground-truth label helps link prediction in heterogeneous graphs,” in *Proceedings of the 2023 2nd International Conference on Algorithms, Data Mining, and Information Technology*, 2023, pp. 6–12.
- [41] W. Jin, Y. Ma, X. Liu, X. Tang, S. Wang, and J. Tang, “Graph structure learning for robust graph neural networks,” in *Proceedings of the 26th ACM SIGKDD international conference on knowledge discovery & data mining*, 2020, pp. 66–74.
- [42] Y. Chen, L. Wu, and M. Zaki, “Iterative deep graph learning for graph neural networks: Better and robust node embeddings,” *Advances in neural information processing systems*, vol. 33, pp. 19314–19326, 2020.

- [43] Q. Sun, J. Li, H. Peng, J. Wu, X. Fu, C. Ji, and S. Y. Philip, "Graph structure learning with variational information bottleneck," in *Proceedings of the AAAI Conference on Artificial Intelligence*, vol. 36, no. 4, 2022, pp. 4165–4174.
- [44] Y. Liu, Y. Zheng, D. Zhang, H. Chen, H. Peng, and S. Pan, "Towards unsupervised deep graph structure learning," in *Proceedings of the ACM Web Conference 2022*, 2022, pp. 1392–1403.
- [45] X. Wang, M. Zhu, D. Bo, P. Cui, C. Shi, and J. Pei, "Am-gcn: Adaptive multi-channel graph convolutional networks," in *Proceedings of the 26th ACM SIGKDD International conference on knowledge discovery & data mining*, 2020, pp. 1243–1253.
- [46] D. Yu, R. Zhang, Z. Jiang, Y. Wu, and Y. Yang, "Graph-revised convolutional network," in *Machine Learning and Knowledge Discovery in Databases: European Conference, ECML PKDD 2020, Ghent, Belgium, September 14–18, 2020, Proceedings, Part III*. Springer, 2021, pp. 378–393.
- [47] C. Zheng, B. Zong, W. Cheng, D. Song, J. Ni, W. Yu, H. Chen, and W. Wang, "Robust graph representation learning via neural sparsification," in *International Conference on Machine Learning*. PMLR, 2020, pp. 11 458–11 468.
- [48] L. Yang, Z. Kang, X. Cao, D. J. 0001, B. Yang, and Y. Guo, "Topology optimization based graph convolutional network." in *IJCAI*, 2019, pp. 4054–4061.
- [49] J. Zhao, X. Wang, C. Shi, B. Hu, G. Song, and Y. Ye, "Heterogeneous graph structure learning for graph neural networks," in *Proceedings of the AAAI conference on artificial intelligence*, vol. 35, no. 5, 2021, pp. 4697–4705.
- [50] W. Bi, L. Du, Q. Fu, Y. Wang, S. Han, and D. Zhang, "Make heterophilic graphs better fit gnn: A graph rewiring approach," *IEEE Transactions on Knowledge and Data Engineering*, 2024.
- [51] H. Kenlay, D. Thanos, and X. Dong, "On the stability of graph convolutional neural networks under edge rewiring," in *ICASSP 2021-2021 IEEE International Conference on Acoustics, Speech and Signal Processing (ICASSP)*. IEEE, 2021, pp. 8513–8517.
- [52] Y. Rong, W. Huang, T. Xu, and J. Huang, "Dropedge: Towards deep graph convolutional networks on node classification," *arXiv preprint arXiv:1907.10903*, 2019.
- [53] J. Li, S. Tian, R. Wu, L. Zhu, W. Zhao, C. Meng, L. Chen, Z. Zheng, and H. Yin, "Less can be more: Unsupervised graph pruning for large-scale dynamic graphs," *arXiv preprint arXiv:2305.10673*, 2023.
- [54] B. S. Lawrence and N. P. Shah, "Homophily: Measures and meaning," *Academy of Management Annals*, vol. 14, no. 2, pp. 513–597, 2020.
- [55] P. Natekar and M. Sharma, "Representation based complexity measures for predicting generalization in deep learning," *arXiv preprint arXiv:2012.02775*, 2020.
- [56] D. L. Davies and D. W. Bouldin, "A cluster separation measure," *IEEE transactions on pattern analysis and machine intelligence*, no. 2, pp. 224–227, 1979.
- [57] R. A. Fisher, "The use of multiple measurements in taxonomic problems," *Annals of eugenics*, vol. 7, no. 2, pp. 179–188, 1936.
- [58] W. Y. Wang, "'liar, liar pants on fire': A new benchmark dataset for fake news detection," *arXiv preprint arXiv:1705.00648*, 2017.
- [59] A. L. Traud, P. J. Mucha, and M. A. Porter, "Social structure of facebook networks," *Physica A: Statistical Mechanics and its Applications*, vol. 391, no. 16, pp. 4165–4180, 2012.
- [60] J. Tang, J. Sun, C. Wang, and Z. Yang, "Social influence analysis in large-scale networks," in *Proceedings of the 15th ACM SIGKDD international conference on Knowledge discovery and data mining*, 2009, pp. 807–816.
- [61] T. N. Kipf and M. Welling, "Semi-supervised classification with graph convolutional networks," *arXiv preprint arXiv:1609.02907*, 2016.
- [62] P. Veličković, G. Cucurull, A. Casanova, A. Romero, P. Lio, and Y. Bengio, "Graph attention networks," *arXiv preprint arXiv:1710.10903*, 2017.
- [63] D. Lim, F. Hohne, X. Li, S. L. Huang, V. Gupta, O. Bhalerao, and S. N. Lim, "Large scale learning on non-homophilous graphs: New benchmarks and strong simple methods," *Advances in Neural Information Processing Systems*, vol. 34, pp. 20 887–20 902, 2021.
- [64] L. Franceschi, M. Niepert, M. Pontil, and X. He, "Learning discrete structures for graph neural networks," in *International conference on machine learning*. PMLR, 2019, pp. 1972–1982.